ACS APPLIED MATERIALS & INTERFACES

Research Article

www.acsami.org

Controlled Drug Release from the Aggregation−Disaggregation Behavior of pH-Responsive Microgels

Yongfeng Gao,[†] Andrews Ahiabu,[†] and Michael J. Serpe*

Department of Chemistry, University of Alberta, Edmonton, Alberta Canada T6G 2G2

Supporting Information

ABSTRACT: In this submission, two independent sets of microgels were synthesized that exhibit pH responsivity over different solution pH ranges. The microgels were synthesized by copolymerizing two different comonomers with poly(*N*-isopropylacrylamide) (pNIPAm). The microgels copolymerized with acrylic acid exhibit a negative charge above pH 4.25, while the microgels copolymerized with *N*-[3-(dimethylamino)propyl]methacrylamide exhibit a positive charge below pH 8.4; these microgels are neutral outside of these pH ranges. We show that aggregates form when the two independent sets of microgels are exposed to one another in a solution that renders them both charged. Furthermore, in solutions of pH outside of this range, the microgels disaggregate because one of the microgels becomes neutralized. This behavior was exploited to load (aggregation) and release (disaggregation) a small-molecule model drug, methylene blue. This aggregate-based system is one example of how pNIPAm-based microgels can be used for controlled/triggered drug delivery, which can have implications for therapeutics.

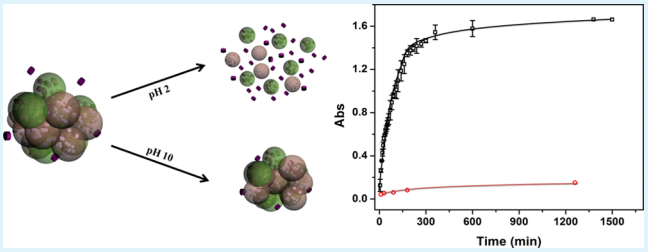

KEYWORDS: *stimuli-responsive polymers, poly(N-isopropylacrylamide)-based microgels, pH-responsive microgels, controlled/triggered drug delivery, electrostatic interactions*

INTRODUCTION

Polymer microgels are colloidally stable cross-linked hydrogel particles that have a swollen network structure in a suitable "good" solvent.[1−4] Microgels have attracted much attention in theoretical studies of soft matter[5−7] and for various applications[8,9] over the past several decades. In particular, they have rapidly gained considerable importance in materials science owing to their potential applications in drug delivery,[10,11] sensing,[12−14] photonic crystal fabrication,[15−17] and separation and purification technologies.[18] Most of these applications are a direct result of their ability to be rendered responsive to external stimuli; i.e., they can be engineered to undergo reversible solvation state changes in response to environmental stimuli such as the pH,[19,20] temperature,[3,21] ionic strength of the surrounding medium,[22] light,[23,24] electric field[25] and magnetic field.[26] The solvation state of the microgels is often a result of the imbalance/balance between repulsive and attractive forces acting in the particles. Small molecules are easily introduced into microgels via copolymerization of functional comonomers into the microgels, or postpolymerization modification, which can lead to these forces and the resultant responsivity.[21,27]

Poly(*N*-isopropylacrylamide) (pNIPAm) is by far the most extensively studied responsive polymer to date.[28,29] It is well-known to be thermoresponsive, exhibiting a lower critical solution temperature (LCST) at ∼32 °C in water. That is, at temperatures below the LCST, the polymer has favorable interactions with water molecules and exists as a solvated, extended random coil. The polymer−polymer interactions become dominant above this temperature, causing the polymer to desolvate and collapse into a dense globular conformation. Furthermore, the transition is fully reversible and can be repeated many times. Because the LCST is close to physiological temperature, pNIPAm-based materials, such as hydrogels and microgels, have been widely exploited in biomedical and biological applications.[30−32]

Like pNIPAm linear chains, pNIPAm-based hydrogel particles (microgels) are able to switch their solvation state from fully water swollen (large diameter) to dehydrated (small diameter) by increasing the water temperature to above the LCST. PNIPAm-based micro- and nanogels are most easily synthesized via free-radical precipitation polymerization.[33,34] This approach is versatile in terms of the variety of chemical modifications that can be made to the microgels by simply adding functional monomers to the reaction solution prior to the initiation. Using this approach, pNIPAm-based microgels with a variety of chemical functionalities have been synthesized.[35,36] The most commonly used comonomer is acrylic acid (AAc),[15] which renders the pNIPAm-*co*-AAc microgel pH-responsive and can also be used to further modify the microgels with other small molecules.[37] The pH responsivity is a result of the pK_a value of the AAc group.

Received: May 22, 2014
Accepted: August 5, 2014
Published: August 13, 2014

That is, the pK_a value for AAc is ∼4.25,[38] so when the pH of the environment is <4.25, the AAc groups are protonated and neutral (although a slight microgel charge can exist depending on the initiator used), and when the pH is >4.25, the microgels are deprotonated and negatively charged. Similarly, positively charged microgels can be obtained by copolymerization with amine-containing comonomers like *N*-[3-(dimethylamino)-propyl]methacrylamide (DMAPMA), whose pK_a is ∼8.4.[39] Therefore, at pH < 8.4, these microgels are positively charged and exhibit attractive electrostatic interactions with negatively charged species,[40,41] while they have minimal interactions with negatively charged species at high pH (>8.4). This behavior is completely reversed for AAc-modified microgels, which exhibit attractive interactions with positively charged species at pH > 4.25. Thus, these microgels are protonated at higher pH and neutral at lower pH.

Stimuli-responsive microgels have been used and developed for drug-delivery systems in the past.[10,42−44] A variety of different stimuli have been engineered into these systems to allow the release of small molecules in a triggered and controlled fashion. The primary triggers for release from microgel-based drug-delivery systems are the temperature and pH. Microgels have been used as drug carriers by exploiting different forces, such as electrostatic,[45] hydrogen-bonding,[46] or bioconjugate interactions.[42] The drug molecules can diffuse out of the microgels by exposure to an external environment that interrupts these interactions. In most of the cases, the drug loading process is complex,[47] and the loading efficiency of the microgels (or microgel-based systems) is typically limited owing to the size of the microgels. In light of this, it is imperative to find a more effective way of minimizing these disadvantages, making microgel-based technologies viable for drug delivery.

In this study, we developed a facile method to entrap a small-molecule model drug, methylene blue (MB), in microgels by aggregating microgels of opposite charges in the presence of MB. PNIPAm-*co*-AAc and pNIPAm-*co*-DMAPMA microgels were used as negatively and positively charged microgel moieties, respectively. The electrostatic interaction between these two microgels (at given pH) can cause the formation of large aggregates and concomitant loading of the drug. Using this approach, we envisage that the drug loading efficiency will be dramatically increased. The pH-triggered aggregation of the microgels and the resultant release of MB from the microgels due to disaggregation at certain pH values were investigated and were shown to be a viable option for a drug-delivery system.

As mentioned above, the microgels used in this study were synthesized via free-radical precipitation polymerization, as previously described.[15] The microgels were composed of functional groups that render them negatively and positively charged at certain pH values, while they are neutral otherwise. This is due to the different pK_a values for AAc (∼4.25) and DMAPMA (∼8.4); therefore, when the pH is below the pK_a value of AAc group, pNIPAm-*co*-AAc microgels are neutral and pNIPAm-*co*-DMAPMA microgels are positively charged, while when the pH of the solution is greater than the pK_a value for DMAPMA, the pNIPAm-*co*-AAc microgels are negatively charged and the pNIPAm-*co*-DMAPMA microgels are neutral. In the range of pH 4.25−8.4, both sets of microgels are charged to different extents, which leads to various degrees of pNIPAm-*co*-AAc/pNIPAm-*co*-DMAPMA microgel aggregation when they are mixed. During aggregation, small-molecule model drugs in the surrounding solution can be trapped inside the aggregates, as depicted in Scheme 1. This phenomenon is in accordance with the scrambled-egg model.[41] In this study, we used the dye molecule MB as a model drug; its structure is shown in Scheme 1. MB is a positively charged molecule, independent of the solution pH.

Scheme 1. Aggregate Formation and Model Drug (MB) Trapping When Microgels Are Mixed at a pH That Renders Them Both Charged

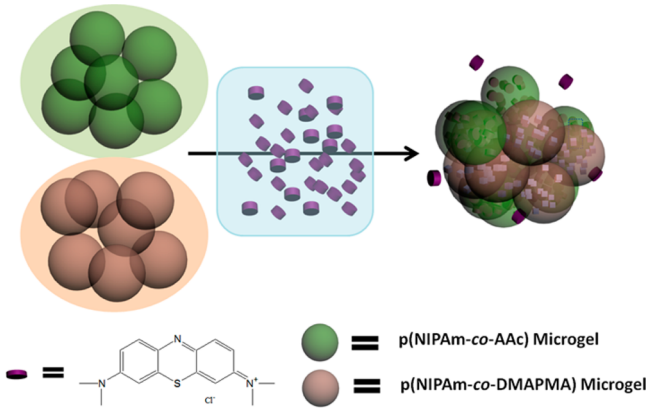

To evaluate the aggregation behavior, the microgels were mixed together at various pH values. A photographic image of the aggregated microgels themselves without MB at different solution pH values is shown in Figure 1. We note that the microgels at pH 2 and 12 do not visually aggregate and the microgel solution remains turbid, indicative of the microgels remaining dispersed in the solution. This is quite different when the microgels are mixed together at pH 5 and 7, where the microgels visually aggregate into large structures. To further investigate the aggregation behavior, their size and morphology were evaluated using scanning electron microscopy (SEM), and the results can be seen in Figure 2. At pH 2 and 12, the SEM images clearly show that the microgels are not aggregated and appear individually on a substrate. However, at pH 5 and 7, large aggregates were formed and the size is around 2 mm × 4 mm, which is big enough to be seen visually. Most of the

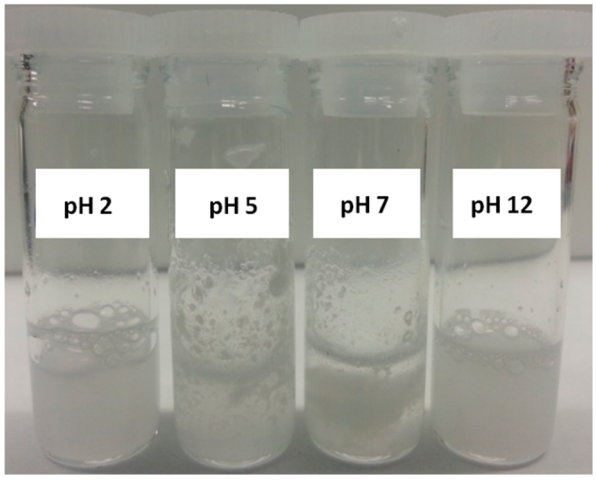

Figure 1. Photograph of microgel-based aggregates in solutions of the indicated pH.

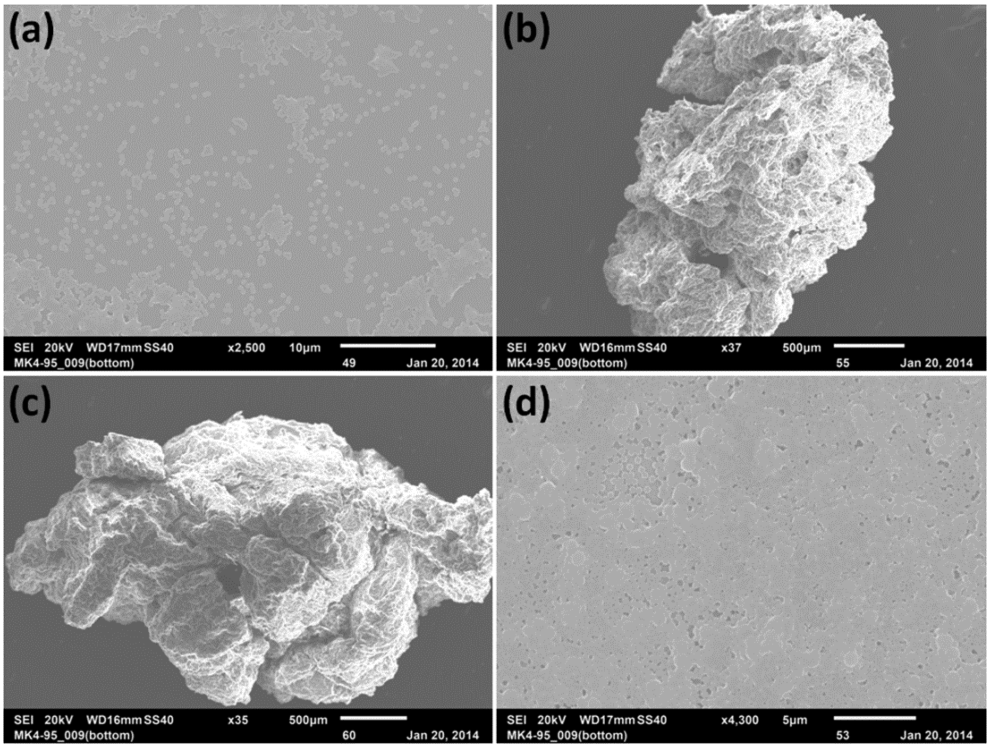

Figure 2. SEM images of samples recovered after two sets of microgels were mixed in solutions of pH (a) 2, (b) 5, (c) 7, and (d) 12.

microgels were involved in the formation of the aggregates, which left the solution less turbid (because there were minimal microgels left unaggregated in the solution). The relative differences in the sizes of the aggregates are shown in the Supporting Information (SI). The SEM images show that the aggregates are tightly bound to one another, which increases their ability to uptake small-molecule model drugs. This is due to the interstices between the aggregated microgels effectively trapping the small molecule, as we have shown previously for water remediation applications.[18,48−50]

When aggregates are formed in the presence of the dye molecule MB, we expect the most efficient trapping at pH 5, 7, and 9, while we expect the least amount of aggregation at pH 2 and 12. To generate the aggregates in the presence of MB, 1.0 mL of a 0.5 mg/mL MB solution was added to individual glass vials and diluted to a total volume of 10 mL with the appropriate pH solution, bringing the final concentration of MB to 0.05 mg/mL. For these experiments, solution pH values of 2, 4, 5, 7, 9, 10, and 12 were used, and the solutions were vivid blue in each case, as can be seen in Figure 3a. Then 50 μL of each microgel, taken directly from a centrifuged microgel pellet (see the Experiment section), was added one at a time to these pH solutions; pNIPAm-*co*-AAc microgels were always added to the solution first followed immediately by pNIPAm-*co*-DMAPMA microgels. The aggregates formed immediately upon the addition of the two microgels to the appropriate pH solution. As can be seen in Figure 3b, the dye was trapped inside the microgels aggregated in solutions of certain pH, as is evidenced by the color of the aggregates and the associated decoloration of the solution. As can be seen from the results, almost no visual aggregates were formed in solutions of pH 2 and 12 (where one of the microgels is neutral, while the other is charged), while large aggregates were formed at pH 5, 7, and 9. Some aggregates were formed at pH 4 and 10 (near the two different pK_a values). This can be explained by the fact that the

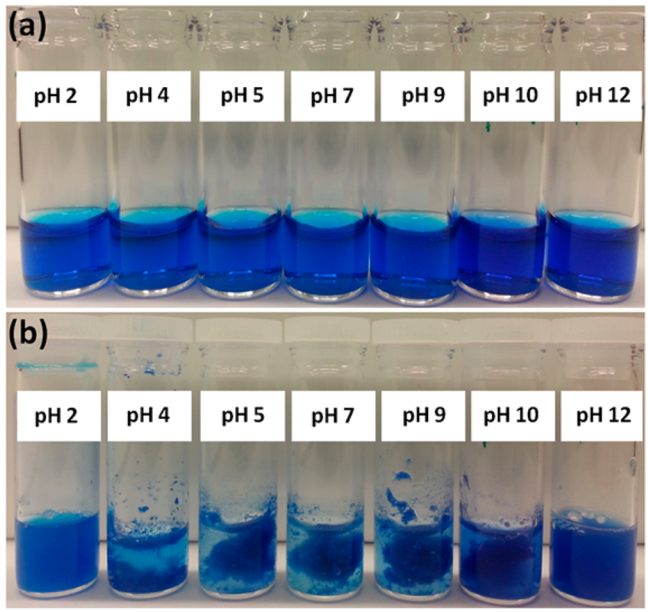

Figure 3. Photographs of MB solutions at the indicated pH (a) before and (b) after the addition and aggregation of the individual sets of microgels.

dissociation constants of the individual comonomers shift in a polymeric system;[51] however, these aggregates were much less efficient at trapping MB. In order to investigate whether the MB dye molecules contribute to the formation of the aggregates, two control experiments were conducted; the results are shown in the SI. The addition of only one set of microgels to MB solutions of various pH values had no effect on the aggregation state of the microgels, meaning that the aggregation is achieved only when the different microgels are together in their charged state.

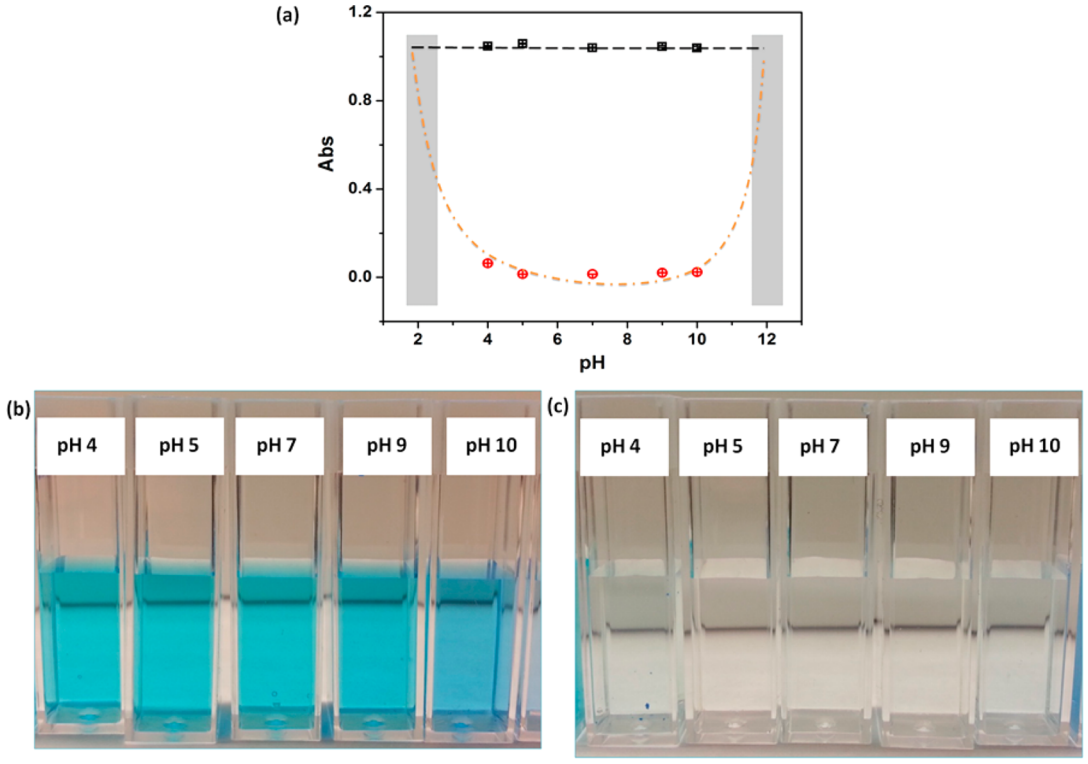

Figure 4. (a) UV−vis absorbance values from MB solutions at the indicated pH (□) before and (○) after microgel aggregation (and removal from solution). Photographs of the remaining solutions at the indicated pH (b) before and (c) after microgel aggregation.

Before the drug release properties of the aggregates were study, the ability of the aggregates to trap MB at the different pH values was further investigated. To do this, the absorbances of MB solutions were measured by UV−vis spectroscopy, before and after aggregates were formed and removed from the MB solutions. Specifically, 200 μL of the MB solution (0.05 mg/mL) was diluted with 2.0 mL of a given pH solution, and the initial absorbance was measured. In this case, we measured the absorbance value at MB's λ_{max} of 664 nm (the full spectrum can be seen in the SI), and the results are shown in Figure 4. As can be seen, the solution pH minimally affects MB's optical properties. Similar to what was observed above, the amount of MB left in solution after aggregation of the microgels depends dramatically on the pH; at pH values where the most efficient aggregation takes place, the most MB is removed from solution. However, the absorbance of the remaining solutions when the "aggregates" were formed at pH 2 and 12 was high because of the excess MB present. It must be noted that pNIPAm-*co*-AAc microgels are negatively charged at high pH, which can allow them to electrostatically bind with MB. However, we have shown that, aggregation has a much greater effect on the uptake than electrostatics alone; see Figure 5. In this case, there are no aggregates formed, but the negative pNIPAm-*co*-AAc microgels will electrostatically interact with positive MB molecules. ζ potential measurements of the individual pNIPAm-*co*-AAc and pNIPAm-*co*-DMAPMA microgels further confirm this aggregation behavior. At the extreme pH values (i.e., pH 2 and 12), only one set of the microgels is charged (for example, pNIPAm-*co*-AAc is negatively charged at pH 12, while pNIPAm-*co*-DMAPMA is positively charged at pH 2, as shown in the shaded region of Figure S4 in the SI). However, at pH ranges between these shaded portions, the two sets of microgels have strong opposite charges, which promotes the formation of aggregates.

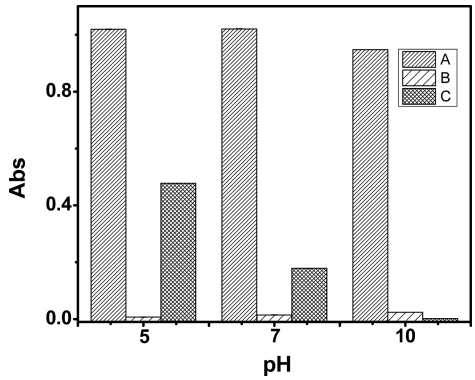

Figure 5. Absorbance values for MB solutions at the indicated pH. MB solutions (A) before the addition of microgels, (B) after microgel aggregation, and (C) after the addition of just the pNIPAm-*co*-AAc microgels alone and centrifugation to remove the microgels from solution. The electrostatic interaction between MB and the pNIPAm-*co*-AAc microgels becomes stronger as the solution pH increases, leading to more uptake of MB and less left over in solution, although, at the pH here, the amount of MB left over in solution after aggregation is the same, indicating that the aggregates are able to trap MB, in addition to the electrostatic interactions.

Next, the ability of the aggregates to release MB at different pH values was investigated. This was done by isolating the aggregates formed at pH 5 and 7 and exposing the aggregates to solutions that have pH values that render one of the sets of microgels neutral. To do this, a glass vessel containing 5.0 mL of aqueous solution (either pH 2 or 10) was placed on a hot plate to control the solution temperature at 25 °C, while the solution was stirred at a rate of 80 rpm. Then a small vial

containing the MB-loaded aggregates was immersed in the glass container such that the liquid filled the small vial and contacted the aggregates. At this point, a timer was started. The whole assembly was covered with a glass slide to prevent the water from evaporating. The aggregates were placed in the small vial to keep them from becoming damaged from the stirring. At given time intervals, 2.0 mL of the solution was removed from the release vessel, and a UV−vis spectrum was acquired. In pH 2, the absorbance was taken every 5 min for the first 1 h, then every 10 min in the second 1 h, and every 20 min in the third 1 h, until the release profile plateaued. In pH 10, the release was slow (due to the AAc charge), so the absorbance was taken at less frequent intervals. Following each UV−vis measurement, all of the liquid was carefully returned to the release vessel. The experimental setup is summarized in Scheme 2, while the

Scheme 2. Schematic Representation of the Drug Release Experimental Setup

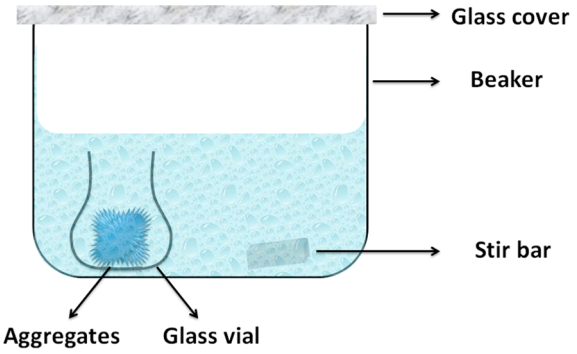

results are shown in Figure 6. Figure 6a shows the release profiles for aggregates formed at pH 5. As can be seen, MB is released very quickly from the aggregates at pH 2, with the release completing in ∼5 h. However, at pH 10, the release was so slow that the absorbance was still lower than 0.2 even after 50 h, which is much slower than the release in pH 2 (the absorbance reached this value in 15 min). Therefore, MB can be released at a rate that is controlled by the pH. Figure 6b shows the same experiments, but for the aggregates formed at pH 7. As can be seen, the same phenomenon was observed for these aggregates: very fast release for the aggregates exposed to pH 2 solution and very slow release at pH 10. When in lower pH (∼2), the electrostatic interaction between microgels disappeared and disaggregation occurred, making diffusion of the MB molecules out of the microgels much easier. At the same time, pNIPAm-*co*-DMAPMA microgels are positively charged at this pH, which will form a repulsive force with the positively charged MB molecules, hence dramatically increasing diffusion of MB out of the microgel aggregates. Therefore, the disaggregation and repulsive forces, in combination with AAc neutralization, are the collective forces that contribute to the faster release at pH 2. However, at pH 10, while the aggregates still broke up because of neutralization of the pNIPAm-*co*-DMAPMA microgels, the pNIPAm-*co*-AAc microgels are fully negatively charged, which causes them to form attractive electrostatic interactions with the MB molecules (Figure 5). This makes the release of MB from the aggregates much slower. The photographs of the solution after release in different pH values are shown in Figure S5 in the SI. We can clearly see that, even after release, the solution color turned blue in pH 2, while it was almost colorless in pH 10.

Following this, we investigated the ability of the aggregates to release MB in a pH-triggered fashion. To investigate this, the aggregates were first immersed in a pH 10 solution and the release profile was measured over ∼4 h. The solution pH was then reduced from pH 10 to 2 by the addition of HCl, and the release was continuously monitored. The results are shown in Figure 7. When the pH was changed from 10 to 2 at 270 min, the absorbance increased immediately, eventually stabilizing at 0.8. This result shows that changing the pH can trigger the release of the model drug MB.

CONCLUSION

In conclusion, we synthesized pH-responsive microgels, which exhibit opposite charges over a given solution pH range. We showed that the microgels aggregated when they were mixed in this pH range, which could be used to trap/load a small-molecule model drug, MB. We showed that the loading efficiency was greater when the microgels aggregated, compared to simply relying on electrostatic interactions for loading. Finally, we showed that the MB could be released in a pH-dependent fashion over many hours/days at certain pH conditions. This is a clear demonstration of how microgel-based technology could be used for health-related applications, which could be used to release biologically relevant molecules at low pH environments typically found at tumor cites.

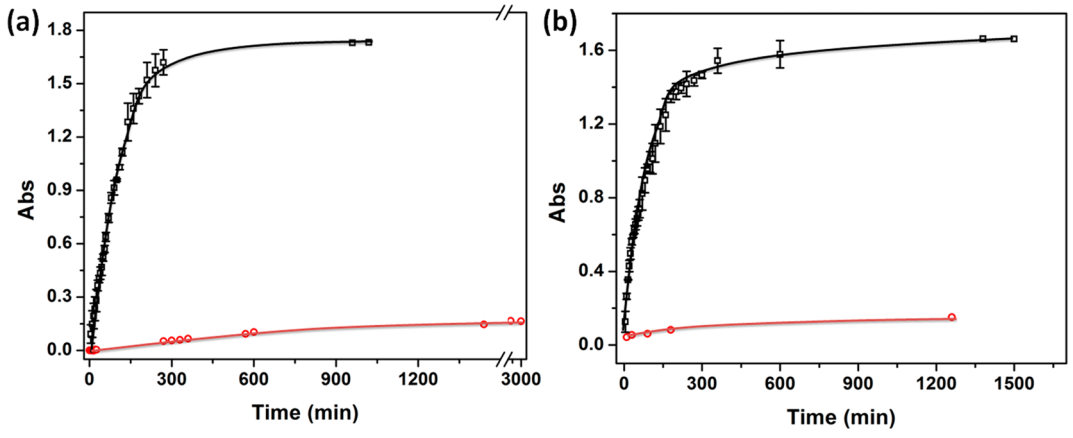

Figure 6. Drug release profiles in (□) pH 2 and (○) pH 10 solutions for aggregates formed at (a) pH 5 and (b) pH 7. Each point is the average for three individual experiments, while the error bars are the standard deviations.

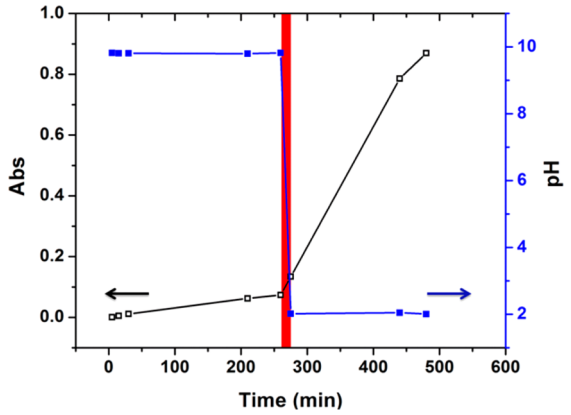

Figure 7. Triggered small-molecule release from the microgel-based aggregates upon a change of the solution pH from 10 to 2 at the time indicated by the shaded region.

EXPERIMENT

Materials. Unless otherwise specified, all reagents were purchased from Sigma-Aldrich. *N*- Isopropylacrylamide (NIPAm) was purified by recrystallization from hexanes prior to use. *N*,*N*′-Methylenebis-(acrylamide) (BIS), acrylic acid (AAc), *N*-[3-(dimethylamnino)-propyl]methacrylamide (DMAPMA), and ammonium persulfate (APS) were used without further purification. Methylene blue (MB) was used as the model drug. A UV−vis spectrometer (Hewlett-Packard diode array spectrometer) was used to monitor the release of the model drug. A pH meter (JENCO 6173 pH) was used to prepare the pH solutions using sodium hydroxide (NaOH) and hydrochloric acid (HCl) to adjust the pH. Millipore water (18.2 MΩ·cm) from a Milli-Q Plus system (Fisher, Z00QSVC01) was used in this experiment. A scanning electron microscope (JSM-6010LA, JEOL, Peabody, MA) was used to image the aggregates.

Synthesis of Microgels. *pNIPAm-co-AAc.* The microgels were synthesized following a previously published procedure.[15,19] A three-neck flask was fitted with a reflux condenser, nitrogen inlet, and temperature probe and charged with a solution of NIPAm (11.9 mmol) and BIS (0.703 mmol) in 99 mL of deionized water, previously filtered through a 0.2 μm filter. The solution was purged with N_2 and allowed to heat to 70 °C for 1.5 h. AAc (1.43 mmol) was added to the heated reaction mixture in one aliquot, immediately initiating the reaction with a solution of APS (0.2 mmol) in 1 mL of deionized water. The reaction was then allowed to proceed at 70 °C for 4 h under a blanket of N_2. The resulting suspension was allowed to cool overnight and filtered through Whatman No. 1 filter paper to remove any large aggregates. The microgel solution was then distributed into centrifuge tubes and purified via centrifugation at ∼10000 rpm for ∼30 min to form a pellet, followed by removal of the supernatant and resuspension in deionized water six times.

pNIPAm-co-DMAPMA. These microgels were synthesized similarly to the above protocol. A three-neck flask was fitted with a reflux condenser, nitrogen inlet, and temperature probe and charged with a solution of NIPAm (11.9 mmol) and BIS (0.703 mmol) in 99 mL of deionized water, previously filtered through a 0.2 μm filter. The solution was purged with N_2 and allowed to heat to 70 °C for 1.5 h. DMAPMA (1.43 mmol) was added to the heated reaction mixture in one aliquot, immediately initiating the reaction with a solution of APS (0.2 mmol) in 1 mL of deionized water. The reaction was then allowed to proceed at 70 °C for 2 h under a blanket of N_2. The resulting suspension was allowed to cool overnight and filtered through a pad of glass wool to remove any large aggregates. The microgel solution was then distributed into centrifuge tubes and purified via centrifugation at ∼10000 rpm for ∼30 min to form a pellet, followed by removal of the supernatant and resuspension in deionized water six times.

Aggregation of Microgels. A 1:1 (v/v) ratio (50:50 μL) of concentrated microgels of pNIPAm-*co*-AAc and pNIPAm-*co*-DMAPMA were mixed in a glass vial containing 1.0 mL of pH solutions (pH 2, 4, 5, 7, 9, 10, and 12). The pH solutions were prepared using HCl and NaOH with the ionic strength (IS) adjusted to 2.0 mM using NaCl.

UV−Vis Spectroscopy. The absorbance of the supernatant solutions from the aggregation studies was measured. In each case, 200 μL of the supernatant from all pH solutions was diluted with 2000 μL of a solution with the same pH.

Drug Release. Efficient aggregation was observed for microgels mixed at pH 5 and 7, so the drug was loaded in solutions of this pH and released at pH 2 and 10 (where no or few aggregates were observed). The aggregated microgels were kept in a vial, placed in a beaker containing 5 mL of either pH 2 or 10 solutions, and covered. The temperature was set to 25 °C and with a stirring rate of 80 rpm. The release of the drug was monitored every 5 min for 1 h, every 10 min for another 1 h, and finally every 20 min until the release profile plateaued. We showed the controlled release of the drug by loading the drug at pH 5 and releasing at pH 10 for 4 h, after which 0.1 M HCl was added to drop the pH of the solution from 10 to 2, monitoring the release for another 4 h.

Characterization of Aggregates. SEM was done on aggregates formed in solutions of different pH values. The samples were taken from pH 2, 5, 7, and 12 and dried for 2 days. Before SEM was performed, samples were coated with a ∼10 nm layer of gold by sputtering.

ζ Potential Measurement. The ζ potentials of the individual microgels were measured at different pH solutions using a Malvern Zetasizer Nano ZS instrument (Malvern, UK) with a 633 nm laser at 25 °C. Briefly, about 2 μL of each concentrated microgel pellet was dispersed in 1000 μL of a pH solution (IS 2.0 mM). A total of 500 μL of these solutions was used for the ζ potential measurement.

ASSOCIATED CONTENT

Supporting Information

SEM images showing the relative aggregate sizes of the microgels at different pH values, control experiment with the individual microgels at different pH values, UV−vis absorption spectrum for MB at pH 5 and 10, ζ potential measurement of individual microgels at different pH values, and photograph showing the release of MB from the aggregates at pH 2 and 10. This material is available free of charge via the Internet at http://pubs.acs.org.

AUTHOR INFORMATION

Corresponding Author

*E-mail: michael.serpe@ualberta.ca.

Author Contributions

†The authors contributed equally to this work.

Notes

The authors declare no competing financial interest.

ACKNOWLEDGMENTS

M.J.S. acknowledges funding from the University of Alberta (Department of Chemistry and Faculty of Science), the Natural Sciences and Engineering Research Council of Canada, the Canada Foundation for Innovation, and the Alberta Advanced Education & Technology Small Equipment Grants Program.

REFERENCES

(1) Eydelnant, I. A.; Li, B. B.; Wheeler, A. R. Microgels On-Demand. *Nat. Commun.* **2014**, *5*, 1−9.

(2) Zhang, J.; Xu, S.; Kumacheva, E. Polymer Microgels: Reactors for Semiconductor, Metal, and Magnetic Nanoparticles. *J. Am. Chem. Soc.* **2004**, *126*, 7908−7914.

(3) Pelton, R. Temperature-Sensitive Aqueous Microgels. *Adv. Colloid Interface Sci.* **2000**, *85*, 1−33.

(4) Senff, H.; Richtering, W. Temperature Sensitive Microgel Suspensions: Colloidal Phase Behavior and Rheology of Soft Spheres. *J. Chem. Phys.* **1999**, *111*, 1705−1711.
(5) Mezzenga, R.; Schurtenberger, P.; Burbidge, A.; Michel, M. Understanding Foods as Soft Materials. *Nat. Mater.* **2005**, *4*, 729−740.
(6) Nayak, S.; Lyon, L. A. Soft Nanotechnology with Soft Nanoparticles. *Angew. Chem., Int. Ed.* **2005**, *44*, 7686−7708.
(7) Heyes, D.; Brańka, A. Interactions between Microgel Particles. *Soft Matter* **2009**, *5*, 2681−2685.
(8) Mattsson, J.; Wyss, H. M.; Fernandez-Nieves, A.; Miyazaki, K.; Hu, Z.; Reichman, D. R.; Weitz, D. A. Soft Colloids make Strong Glasses. *Nature* **2009**, *462*, 83−86.
(9) Saunders, B. R.; Vincent, B. Microgel Particles as Model Colloids: Theory, Properties and Applications. *Adv. Colloid Interface Sci.* **1999**, *80*, 1−25.
(10) Oh, J. K.; Lee, D. I.; Park, J. M. Biopolymer-Based Microgels/Nanogels for Drug Delivery Applications. *Prog. Polym. Sci.* **2009**, *34*, 1261−1282.
(11) Malmsten, M. Microgels in Drug Delivery. In *Microgel Suspensions: Fundamentals and Applications*; Fernandez-Nieves, A., Wyss, H. M., Mattsson, J., Weitz, D. A., Eds.; Wiley-VCH Verlag GmbH & Co. KGaA: Weinheim, Germany, 2011; pp 375−405.
(12) Hendrickson, G. R.; Lyon, L. A. Bioresponsive Hydrogels for Sensing Applications. *Soft Matter* **2009**, *5*, 29−35.
(13) Su, S.; Ali, M. M.; Filipe, C. D.; Li, Y.; Pelton, R. Microgel-Based Inks for Paper-Supported Biosensing Applications. *Biomacromolecules* **2008**, *9*, 935−941.
(14) Islam, M. R.; Serpe, M. J. Polyelectrolyte Mediated Intra and Intermolecular Crosslinking in Microgel-Based Etalons for Sensing Protein Concentration in Solution. *Chem. Commun.* **2013**, *49*, 2646−2648.
(15) Sorrell, C. D.; Carter, M. C.; Serpe, M. J. Color Tunable Poly(*N*-Isopropylacrylamide)-*co*-Acrylic Acid Microgel−Au Hybrid Assemblies. *Adv. Funct. Mater.* **2011**, *21*, 425−433.
(16) Lyon, L. A.; Debord, J. D.; Debord, S. B.; Jones, C. D.; McGrath, J. G.; Serpe, M. J. Microgel Colloidal Crystals. *J. Phys. Chem. B* **2004**, *108*, 19099−19108.
(17) Debord, J. D.; Lyon, L. A. Thermoresponsive Photonic Crystals. *J. Phys. Chem. B* **2000**, *104*, 6327−6331.
(18) Parasuraman, D.; Serpe, M. J. Poly(*N*-Isopropylacrylamide) Microgels for Organic Dye Removal from Water. *ACS Appl. Mater. Interfaces* **2011**, *3*, 2732−2737.
(19) Debord, J. D.; Lyon, L. A. Synthesis and Characterization of pH-Responsive Copolymer Microgels with Tunable Volume Phase Transition Temperatures. *Langmuir* **2003**, *19*, 7662−7664.
(20) Garcia, A.; Marquez, M.; Cai, T.; Rosario, R.; Hu, Z.; Gust, D.; Hayes, M.; Vail, S. A.; Park, C.-D. Photo-, Thermally, and pH-Responsive Microgels. *Langmuir* **2007**, *23*, 224−229.
(21) Hoare, T.; Pelton, R. Highly pH and Temperature Responsive Microgels Functionalized with Vinylacetic Acid. *Macromolecules* **2004**, *37*, 2544−2550.
(22) Zhao, B.; Moore, J. S. Fast pH-and Ionic Strength-Responsive Hydrogels in Microchannels. *Langmuir* **2001**, *17*, 4758−4763.
(23) Dai, S.; Ravi, P.; Tam, K. C. Thermo-and Photo-Responsive Polymeric Systems. *Soft Matter* **2009**, *5*, 2513−2533.
(24) Zhang, Q. M.; Xu, W.; Serpe, M. J. Optical Devices Constructed from Multiresponsive Microgels. *Angew. Chem., Int. Ed.* **2014**, *53*, 4827−4831.
(25) Klinger, D.; Landfester, K. Stimuli-Responsive Microgels for the Loading and Release of Functional Compounds: Fundamental Concepts and Applications. *Polymer* **2012**, *53*, 5209−5231.
(26) Brugger, B.; Richtering, W. Magnetic, Thermosensitive Microgels as Stimuli-Responsive Emulsifiers Allowing for Remote Control of Separability and Stability of Oil in Water Emulsions. *Adv. Mater.* **2007**, *19*, 2973−2978.
(27) Nayak, S.; Lyon, L. A. Ligand-Functionalized Core/Shell Microgels with Permselective Shells. *Angew. Chem., Int. Ed.* **2004**, *43*, 6706−6709.
(28) Heskins, M.; Guillet, J. E. Solution Properties of Poly(*N*-isopropylacrylamide). *J. Macromol. Sci., Chem.* **1968**, *2*, 1441−1455.
(29) Fujishige, S.; Kubota, K.; Ando, I. Phase Transition of Aqueous Solutions of Poly(*N*-isopropylacrylamide) and Poly(*N*-isopropylmethacrylamide). *J. Phys. Chem.* **1989**, *93*, 3311−3313.
(30) Okano, T.; Yamada, N.; Sakai, H.; Sakurai, Y. A Novel Recovery System for Cultured Cells using Plasma-Treated Polystyrene Dishes Grafted with Poly(*N*-isopropylacrylamide). *J. Biomed. Mater. Res.* **1993**, *27*, 1243−1251.
(31) Hoare, T.; Santamaria, J.; Goya, G. F.; Irusta, S.; Lin, D.; Lau, S.; Padera, R.; Langer, R.; Kohane, D. S. A Magnetically Triggered Composite Membrane for On-Demand Drug Delivery. *Nano Lett.* **2009**, *9*, 3651−3657.
(32) Kost, J.; Langer, R. Responsive Polymeric Delivery Systems. *Adv. Drug Delivery Rev.* **2012**, *64*, 327−341.
(33) Wu, X.; Pelton, R.; Hamielec, A.; Woods, D.; McPhee, W. The Kinetics of Poly(*N*-isopropylacrylamide) Microgel Latex Formation. *Colloid Polym. Sci.* **1994**, *272*, 467−477.
(34) Jones, C. D.; Lyon, L. A. Shell-Restricted Swelling and Core Compression in Poly(*N*-isopropylacrylamide) Core−Shell Microgels. *Macromolecules* **2003**, *36*, 1988−1993.
(35) Hoare, T.; Pelton, R. Engineering Glucose Swelling Responses in Poly(*N*-isopropylacrylamide)-Based Microgels. *Macromolecules* **2007**, *40*, 670−678.
(36) Das, M.; Sanson, N.; Kumacheva, E. Zwitterionic Poly(betaine-*n*-isopropylacrylamide) Microgels: Properties and Applications. *Chem. Mater.* **2008**, *20*, 7157−7163.
(37) Sorrell, C. D.; Serpe, M. J. Glucose Sensitive Poly(*N*-isopropylacrylamide) Microgel Based Etalons. *Anal. Bioanal. Chem.* **2012**, *402*, 2385−2393.
(38) Johnson, K. C.; Mendez, F.; Serpe, M. J. Detecting Solution pH Changes using Poly(*N*-isopropylacrylamide)-*co*-Acrylic Acid Microgel-Based Etalon Modified Quartz Crystal Microbalances. *Anal. Chim. Acta* **2012**, *739*, 83−88.
(39) Eke, I.; Elmas, B.; Tuncel, M.; Tuncel, A. A new, Highly Stable Cationic-Thermosensitive Microgel: Uniform Isopropylacrylamide−dimethylaminopropylmethacrylamide Copolymer Particles. *Colloids Surf., A* **2006**, *279*, 247−253.
(40) Suzuki, D.; Horigome, K. Binary Mixtures of Cationic and Anionic Microgels. *Langmuir* **2011**, *27*, 12368−12374.
(41) Kaur, J.; Harikumar, S. L.; Kaur, A. Interpolyelectrolyte Complexes as Prospective Carriers for Controlled Drug Delivery. *Int. Res. J. Pharm.* **2012**, *3*, 58−62.
(42) Oh, J. K.; Drumright, R.; Siegwart, D. J.; Matyjaszewski, K. The Development of Microgels/Nanogels for Drug Delivery Applications. *Prog. Polym. Sci.* **2008**, *33*, 448−477.
(43) Soppimath, K.; Aminabhavi, T.; Dave, A.; Kumbar, S.; Rudzinski, W. Stimulus-Responsive "Smart" Hydrogels as Novel Drug Delivery Systems. *Drug Dev. Ind. Pharm.* **2002**, *28*, 957−974.
(44) Zha, L.; Banik, B.; Alexis, F. Stimulus Responsive Nanogels for Drug Delivery. *Soft Matter* **2011**, *7*, 5908−5916.
(45) Gao, Y.; Zago, G. P.; Jia, Z.; Serpe, M. J. Controlled and Triggered Small Molecule Release from a Confined Polymer Film. *ACS Appl. Mater. Interfaces* **2013**, *5*, 9803−9808.
(46) Hoare, T. R.; Kohane, D. S. Hydrogels in Drug Delivery: Progress and Challenges. *Polymer* **2008**, *49*, 1993−2007.
(47) Kakde, D.; Jain, D.; Shrivastava, V.; Kakde, R.; Patil, A. T. Cancer Therapeutics—Opportunities, Challenges and Advances in Drug Delivery. *J. Appl. Pharm. Sci.* **2011**, *01*, 01−10.
(48) Parasuraman, D.; Sarker, A. K.; Serpe, M. J. Poly(*N*-Isopropylacrylamide)-Based Microgels and Their Assemblies for Organic-Molecule Removal from Water. *ChemPhysChem* **2012**, *13*, 2507−2515.
(49) Parasuraman, D.; Leung, E.; Serpe, M. J. Poly(*N*-isopropylacrylamide) Microgel Based Assemblies for Organic Dye Removal from Water: Microgel Diameter Effects. *Colloid Polym. Sci.* **2012**, *290*, 1053−1064.

(50) Parasuraman, D.; Sarker, A. K.; Serpe, M. J. Recyclability of Poly(*N*-isopropylacrylamide) Microgel-Based Assemblies for Organic Dye Removal from Water. *Colloid Polym. Sci.* **2013**, *291*, 1795−1802.
(51) Rmaile, H. H.; Schlenoff, J. B. "Internal pKa's" in Polyelectrolyte Multilayers: Coupling Protons and Salt. *Langmuir* **2002**, *18*, 8263−8265.